Efficient Fast-Convolution Based Implementation of 5G Waveform Processing Using Circular Convolution Decomposition

AlaaEddin Loulou, Juha Yli-Kaakinen, and Markku Renfors
Department of Electronics and Communication Engineering
Tampere University of Technology
Email: {alaa.loulou, juha.yli-kaakinen, markku.renfors}@tut.fi

***Abstract*—Multirate fast convolution (FC) has recently been introduced as an effective tool for communication waveform processing, especially for advanced multicarrier systems targeting at well-contained spectrum. These include filter bank based multicarrier waveforms and filtered OFDM schemes which are receiving increasing attention in the 5G radio access development. Recalling that the key idea of FC is effective implementation of high-order linear filtering through frequency-domain processing, this paper investigates possibilities to reduce the complexity of FC based waveforms. Special focus is on scenarios where a relatively small part of the bandwidth is in active use, which could be the case, e.g., in low-rate machine-type communication devices. A new variant of fast-convolution filter bank (FC-FB) is developed which uses circular convolution decomposition. The narrowband variant of decomposed structure, called D-FC-FB, achieves significantly reduced complexity, which is proportional to the active bandwidth, while maintaining filtering performance equivalent to FC-FB. Therefore, this variant is considered as a low-complexity solution for low-rate devices. D-FC-FB can be used in any multicarrier scheme that utilizes filtering at subcarrier or resource block level. This paper develops closed-form complexity expressions for the case of filter bank multicarrier with offset-QAM subcarrier modulation (FBMC/OQAM) demonstrating significant complexity reduction in a case study.**

I. Introduction

The next mobile generation (5G) brings new challenges to the mobile network due to the newly defined services supporting hundreds of megabits per second user data rates on one hand, and connecting massive number of low-rate devices/machines on the other [1]. The cyclic prefix orthogonal frequency division multiplexing (CP-OFDM) is the current transmission scheme in broadband mobile networks [2]. In order to maintain orthogonality of subcarriers, OFDM requires tight synchronization in time and frequency. This makes it difficult to utilize different numerologies (subcarrier spacings, CP-lengths, etc.) depending on the service and user requirements, which is considered as an important element in the 5G developments. With mixed numerology or in asynchronous spectrum use, CP-OFDM scheme leaks high-powered sidelobes in a wide range around the active subcarriers of a user [3], necessitating wide guardbands in such scenarios.

In the literature, various modulation schemes have been proposed as candidates for 5G to overcome these limitations. Filter bank multicarrier (FBMC/OQAM, also known as OFDM/OQAM) scheme has been widely considered. FBMC delivers high spectral containment for subcarriers using high-order bandpass filters, implemented effectively as a polyphase filter bank [4], [5]. Later, frequency spreading-FBMC (FS-FBMC) has been proposed in [6] providing extra flexibility in controlling the filter frequency responses and simplifying the equalization process. Fast-convolution filter bank (FC-FB) introduced in [7], [8] provides a generalized variant of FS-FBMC, making it possible to significantly reduce the computational complexity, with the cost of controllable increase of in-band and out-of-band interference levels. Besides, the FC-FB scheme is extremely flexible in terms of configuring the subband bandwidths and positions. Moreover, the scheme has shown significant capability in handling heterogeneous scenarios [9] and it provides efficient frequency-domain equalization process [10]. Also other solutions have been proposed for 5G, such as generalized frequency division multiplexing (GFDM) [11] and its FC variant [12] and resource block filtered-OFDM (F-OFDM) [13] and its FC variant [14]. The FC-FB approach provides efficient implementation for all these schemes, resulting in similar increase in computational complexity with respect to CP-OFDM, typically two to four times increased multiplication rate.

In this paper, we propose a novel decomposed FC-FB (D-FC-FB) waveform processing approach. The complexity of the generic full-band D-FC-FB is slightly higher than that of the direct FC-FB scheme, while maintaining identical output. Nevertheless, in narrowband cases where less than 1/8 of the available frequency band is in active use, significant reduction in the complexity can be achieved by pruning the unnecessary parts of the decomposed structure. This scheme is considered as an effective candidate for narrowband transmission scenarios with all the mentioned waveform alternatives.

This paper is arranged as follows. Section II presents the generic idea of the circular convolution (CC) decomposition process. Section III discusses the background of the FC-FB and its parametrization. Section IV proposes first the generic variant of D-FC-FB. Then narrowband variants of D-FC-FB are introduced. Section V discusses the complexity of the D-FC-FB and provides the computational complexity formulas. Section VI compares the computational complexity of D-FC-FB with different transmission waveforms. Finally, the concluding remarks are presented in Section VII.

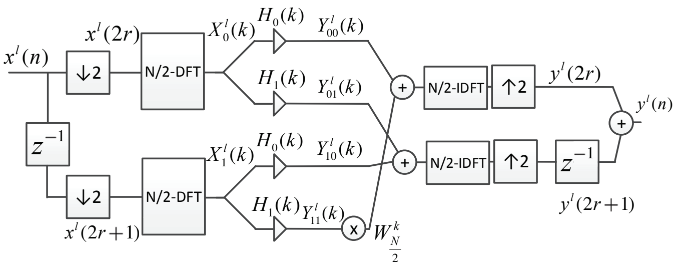

Fig. 1. Decomposition of circular convolution with the factor of $D = 2$.

II. The decomposition of circular convolution

For fixed filter impulse response, the CC consists of taking the discrete Fourier transform (DFT) of the input data block, multiplying the DFT-domain data blocks by the weight coefficients derived from the filter impulse response through DFT, and taking inverse discrete Fourier transform (IDFT) of the result. CC is expressed in DFT domain as follows,

$$y^l[n] = \frac{1}{N}\sum_{k=0}^{N-1} X^l[k]H[k]W_N^{-nk} \tag{1}$$

where N is the size of DFT and IDFT, $W_N = \exp\big[-\frac{2\pi j}{N}\big]$, n is the time index, k is the frequency index, l is the block index, $X^l[k]$ is the DFT of the lth input block $x^l[n]$ and $H[k]$ is the DFT of the filter impulse response $h[n]$. The processes of the decomposed CC, or what is called multi-dimensional circular convolution in [15], starts with dividing the input and the filter in time domain into $D = 2^m$ delay branches, where m is positive integer such the D is a factor of N. Subsequently, the DFTs for both the decimated inputs of the delay branches and the corresponding filter responses are obtained as follows,

$$X_{d_x}^l[k] = \sum_{r=0}^{\frac{N}{D}-1} x^l[rD + d_x]W_{\frac{N}{D}}^{rk} \tag{2}$$

$$H_{d_h}[k] = \sum_{r=0}^{\frac{N}{D}-1} h[rD + d_h]W_{\frac{N}{D}}^{rk} \tag{3}$$

where $d_x = 0, 1, \ldots, D-1$ is the delay index of the input, $d_h = 0, 1, \ldots, D-1$ is the delay index of the filter and r is the decimated time index. Then, partial CC is defined as follows,

$$y_{d_x d_h}^l[n] = \frac{1}{N}\sum_{k=0}^{N-1} Y_{d_x d_h}^l[k]W_N^{(d_x+d_h)k}W_N^{-nk} \tag{4}$$

where $Y_{d_x d_h}^l[k] = X_{d_x}^l[k]H_{d_h}[k]$. The decomposition of (4) by D results in the following,

$$y_{d_x d_h}^l[Dr + d_y] = \frac{D}{N}\sum_{k=0}^{\frac{N}{D}-1} Y_{d_x d_h}^l[k]W_{\frac{N}{D}}^{-k\left(r-\left\lfloor\frac{d_x+d_h}{D}\right\rfloor\right)} \tag{5}$$

where d_x and d_h satisfy the following condition,

$$d_y = (d_x + d_h)_D \tag{6}$$

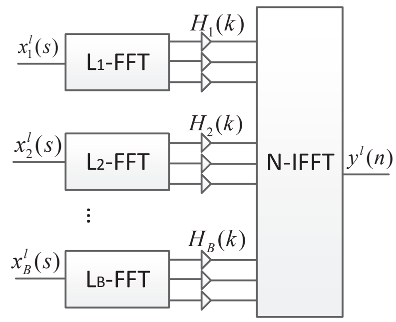

Fig. 2. The generic implementation of FC-FB based SFB without considering the OS process.

where $(\cdot)_D$ denotes the modulo D operation and d_y is the index of the output delay branch. Then the CC outputs are collected from the decimated branches as follows,

$$y^l[Dr + d_y] = \sum_{d_h=0}^{D-1} y_{d_x d_h}^l[Dr + d_y] \tag{7}$$

where d_x satisfies condition of (6). Accordingly, the CC can be performed by obtaining the DFTs of the decimated and delayed inputs $x^l[rD + d_x]$ and filters $h[rD + d_h]$ for each delay branch. Then the decimated outputs are obtained by multiplying the frequency components that satisfy (6). According to (7), the CC of (1) is finally obtained by upsampling and combining the delay branch outputs. Fig. 1 depicts an example of the decomposed CC when $D = 2$.

III. Fast-convolution filter bank

FC is a process to implement linear convolution through overlapping CC, which are implemented effectively in the DFT domain using fast Fourier transform (FFT). The generic structure of FC-FB based synthesis filter bank (SFB) is shown in Fig 2. There are B low-rate input signals denoted as $x_b^l(s)$ where $b = 1, 2, \ldots, B$ is the subband index and $s = 0, 1, \ldots, L_b - 1$ is the low-rate time index. The DFT-domain representations of the subband signals are obtained by DFT of size L_b (L_b-DFT). Each subband is frequency-shifted by k_b^c DFT bins and then multiplied by the discrete frequency response of the corresponding subband filter $H_b[k]$. Subsequently, the overlapping parts of the subbands are summed and then N-IDFT is applied. The inner part of FC-FB utilizes (1) as follows:

$$y^l[n] = \sum_{k=0}^{N-1}\sum_{b=1}^{B} H_b[k]X_b^l[k + k_b^c]W_N^{-nk}. \tag{8}$$

The (possibly non-integer) sampling rate conversion factor is determined by the transform sizes:

$$R_b = \frac{N}{L_b}. \tag{9}$$

FC-FB uses overlap-and-save (OS) or overlap-and-add (OA) processes to approximate linear convolution, introducing a tolerable amount of circular interference. Further discussions about the implementation of FC-FB and analysis of the circular interference effects can be found in [8].

The overlapping of FC-FB processing blocks is achieved through the buffering of input and output data, while the inner process is a CC process which is independent of the used overlap factor. In the following, we propose modifications to the processing structure of the CC part, and the overlapping nature of the overall scheme is not relevant in these developments.

IV. The decomposition of FC based SFB

A. Generic decomposition scheme

Here, we assume that the low rate input $x_b^l[s]$ is upsampled by R_b and then decomposed by D. Defining R_{min} as the smallest interpolation factor among subbands, the decomposition factor D should follow

$$D \leq R_{min} \tag{10}$$

to preserve the short transform structure of FC-FB. As a result, the delayed branches of $x_{b,d_x}^l[r]$ are zeros, except for the first delay branch. Consequently, the discrete frequency response of the delayed branches of the inputs are expressed as follows:

$$X_{b,d_x}^l[k] = \begin{cases} X_b^l[k], & \text{for } d_x = 0 \\ 0, & \text{for } d_x = 1, 2, \ldots, D-1 \end{cases}. \tag{11}$$

Apparently, each signal has to be multiplied D times by the discrete frequency responses of the decimated and delayed versions of the filter as shown in (5). This can be avoided considering the zero components in the discrete frequency response of the filter. The discrete frequency response of the filter is commonly defined as follows,

$$H_b[k] = H_b^p\left[k - k_b^c - \frac{N}{2R_b}\right] W_N^{-\tau_b k} \tag{12}$$

where τ_b is the sampling phase and $H_b^p(k)$ is the filter zero-phase discrete frequency response. The zero-phase discrete frequency response contains non-zero real components in the period $[-\frac{N}{2R_b}, \frac{N}{2R_b} - 1]$, and zeros elsewhere. The delayed and decimated frequency response of the filter can be simplified if the frequency points are re-indexed according to their positions in the spectrum with respect to the ratio $\frac{N}{D}$. Then the frequency shift can be re-mapped to the following,

$$k_b^c = \Delta \frac{N}{D} + k_c' \tag{13}$$

where $\Delta = \left\lfloor \frac{N}{D} \right\rfloor$ and $k_c' = (k_b^c)_{\frac{N}{D}}$. Accordingly, the discrete frequency response of the decomposed filter is defined as follows,

$$H_{k_c',\Delta}^{d_h}[k'] = \frac{1}{D} W_N^{-k' d_h} W_D^{-d_h(\Delta + A_{k_c'}[k'])} G_{k_c',\Delta}[k'] \tag{14}$$

where $G_{k_c',\Delta}[k']$ is the discrete frequency response of the decomposed filter without considering the twiddle factors that result from the decomposition and it is defined as follows:

$$G_{k_c',\Delta}[k'] = W_N^{-\tau_{k_c',\Delta} k'} W_D^{-\tau_{k_c',\Delta}(\Delta + A_{k_c'}[k'])} H_{k_c',\Delta}[k']. \tag{15}$$

Here, $H_{k_c',\Delta}[k']$ is the circularly shifted version of the $H_{k_c',\Delta}^p[k]$ based on the new re-mapping and it is defined as follows:

$$H_{k_c',\Delta}[k'] = H_{k_c',\Delta}^p\left[k' - k_c' - \frac{N}{2R_{k_c',\Delta}} + \frac{N}{D} A_{k_c'}[k']\right]_{\frac{N}{D}}. \tag{16}$$

$A_{k_c'}[k']$ is a conditional function that is defined as follows:

$$A_{k_c'}[k'] = \begin{cases} 0, & \text{for } k' \geq k_c' \\ 1, & \text{for } k' < k_c' \end{cases}. \tag{17}$$

In the case when the non-zero components of $H_b[k]$ are not overlapping with two spectral sections of $\frac{N}{D}$, $G_{k_c',\Delta}[k']$ is equivalent to $H_b[k]$ because $G_{k_c',\Delta}[k'] = 0$ for $k' < k_c'$. But if there is overlapping, $G_{k_c',\Delta}[k'] \neq 0$ for $k' < k_c'$ due to its circularity. Then $A_{k_c'}[k']$ adds a shift to (16) and phase shift to (15). These shifts make the components of $G_{k_c',\Delta}[k']$ equivalent to the corresponding $H_b[k]$ but circularly shifted around $\frac{N}{D}$. Then, the resulting discrete frequency responses of the input signals and filters in (11) and (14) are substituted in (5). Firstly, the condition in (6) is reduced as follows:

$$d_y = (d_h)_D = d. \tag{18}$$

Accordingly the decimated output is expressed as follows,

$$y_d^l[r] = \frac{D}{N} \sum_{k'=0}^{\frac{N}{D}-1} Y_d^l[k'] W_{\frac{N}{D}}^{-rk'} \tag{19}$$

where $Y_d^l(k')$ is the sum of all filtered input signals and it is defined as follows,

$$Y_d^l[k'] = \frac{1}{D} W_N^{-k'd} \sum_{\substack{\Delta=0 \\ k_c' \in K}}^{D-1} Y_{k_c',\Delta}^l[k'] W_D^{-dA_{k_c'}[k']} W_D^{-\Delta d} \tag{20}$$

where $Y_{k_c',\Delta}^l[k']$ is defined as follows:

$$Y_{k_c',\Delta}^l[k'] = G_{k_c',\Delta}[k'] X_{k_c',\Delta}^l[k' + k_c']. \tag{21}$$

The first stages of D-FC-FB and FC-FB are identical and they consist of B blocks of L_b-DFTs and multiplications by filter weights. By analyzing (20), it can be concluded that the sum over Δ and then the multiplication by $W_D^{-\Delta d}$ is a D-IDFT process. Because (20) is defined with respect to k', then $\frac{N}{D}$ blocks of D-IDFTs are required. Furthermore, D blocks of N/D-IDFTs are required as shown in (19). The inputs of the k'th D-IDFT are originated from the frequency points $\left[k', k' + \frac{N}{D}, \ldots, k' + (D-1)\frac{N}{D}\right]$. Furthermore, the twiddle factor $W_D^{-dA_{k_c'}(k')}$ shifts to the $(k'+1)$th D-IDFT when the subband is overlapping with the next $\frac{N}{D}$ section. Finally, the dth output of the k'th D-IDFT is fed to the k'th input of the dth N/D-IDFT. The generic D-FC-FB is shown in Fig. 3.

B. D-FC-FB in narrowband scenario

In narrowband scenarios, the number of active frequency points is relatively small compared to the available ones in the DFT domain. Therefore, if the number of the active frequency points is small enough, it is possible to prune the D-IDFTs. In

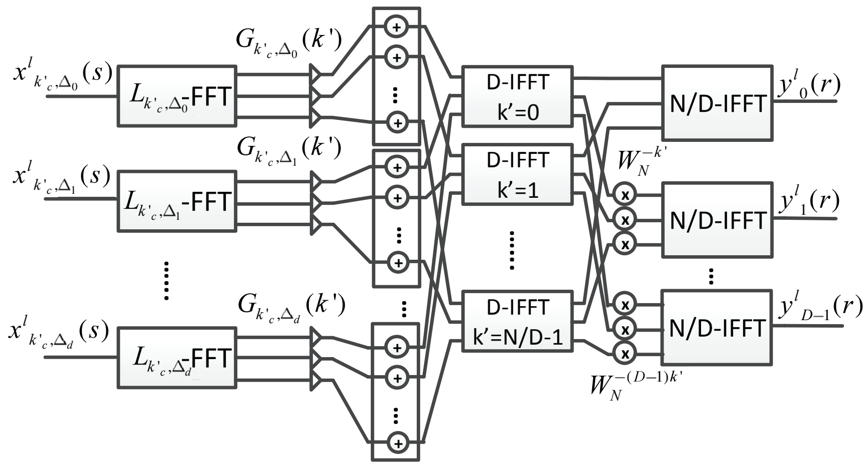

Fig. 3. The generic D-FC-SFB scheme.

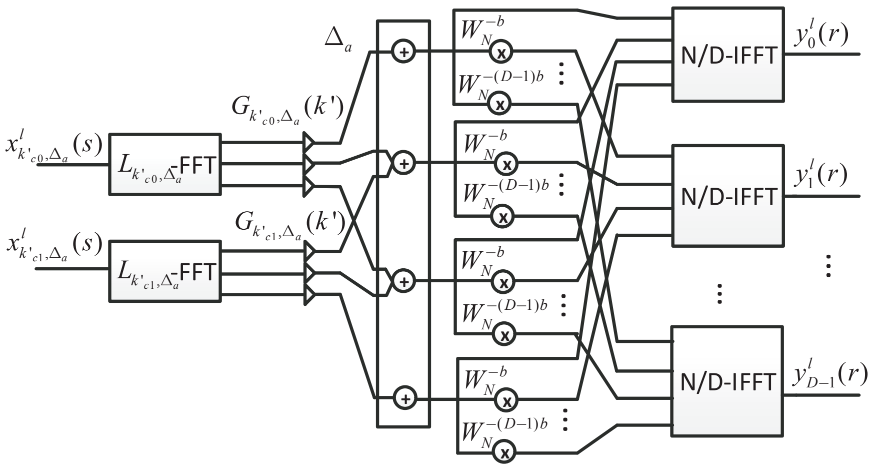

Fig. 4. Narrowband D-FC-FB based SFB, where $b = k' + \frac{N}{D}\Delta_a$.

the considered pruning case the D-IDFTs are having a single non-zero input. In such a case, D-IDFT can be replaced by a series of twiddle factors of $W_D^{-d\Delta}$. This results in two stages of complex multiplication by $W_D^{-d\Delta}$ and $W_N^{-dk'}$, which can be reduced to a single stage of complex multiplication by $W_N^{-d(k'+\frac{N}{D}\Delta)}$. The narrowband D-FC-FB implementation is depicted in Fig. 4.

To achieve a single input pruning, a single non-zero value should be located in frequency slots period of $\left[k', k' + \frac{N}{D}, \ldots, k' + (D-1)\frac{N}{D}\right]$, as shown in Fig. 5. Moreover, the decomposition factor should be,

$$D \leq \frac{N}{N_k} \tag{22}$$

where N_k is the number of used frequency points. The set of used frequency points can be any contiguous set of $N_k \leq \frac{N}{D}$ bins. Also certain non-contiguous sets, following the mentioned rule, are possible.

V. Analysis of the Computational Complexity

Fast Fourier transform (FFT) is an effective implementation of DFT. In this document, the complexity of split-radix FFT is considered, since it is one of the most effective implementation algorithm for FFTs and IFFTs with power-of-two lengths. Its complexity can be expressed as follows [16],

$$\mu_T(N) = N \log_2 N - 3N + 4 \tag{23}$$

$$\alpha_T(N) = 3N \log_2 N - 3N + 4 \tag{24}$$

for number of real multiplications and real additions, respectively. An implementation of the FC schemes contains commonly two parts. The short transforms part that contains B blocks of L_b-FFT, filtering coefficients and the needed block-wise phase rotations (see [8]). This part is common for FC-FB and D-FC-B. The computational complexity of the short

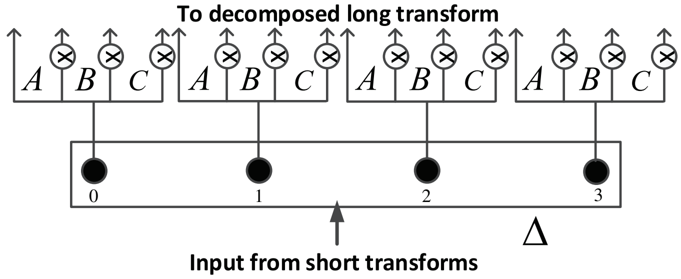

Fig. 5. Example of possible contiguous locations of active frequency points in the narrowband D-FC-FB with $N = 16$ and $D = 4$, where $A = W_D^{-\Delta}$, $B = W_D^{-2\Delta}$ and $C = W_D^{-3\Delta}$.

transforms part is expressed as follows [17], [18],

$$\mu^{sh} = \sum_{b=1}^{B} [\mu_T(L_b) + 2L_{s,b} + 2L_b] \tag{25}$$

$$\alpha^{sh} = 2\theta + \sum_{b=1}^{B} \alpha_T(L_b) \tag{26}$$

where $L_{s,b}$ is the non-overlapping period at the bth input and θ is the total number of overlapping frequency points between subbands. The other part of FC-FB scheme is the long transform part that contains N-IFFT. Therefore, the complexity of this part is directly given by (23) and (24). However, the long transform side of the D-FC-FB requires N/D blocks of D-IFFT and D blocks of N/D-IFFT besides a set of twiddle factors. The complexity of the long transform part is computed as follows:

$$\mu_D^{lg} = \sum_{d=0}^{D-1} \mu_{GT}^d(N, D) + \frac{N}{D}\mu_T(D) \tag{27}$$

$$\alpha_D^{lg} = \sum_{d=0}^{D-1} \alpha_{GT}^d(N, D) + \frac{N}{D}\alpha_T(D). \tag{28}$$

Here $\mu_{GT}^d(N, D)$ and $\alpha_{GT}^d(N, D)$ calculates the required real multiplications and real additions to implement N/D-IFFT with inputs multiplied by $W_N^{-dk'}$ and they are defined as follows,

$$\mu_{GT}^d(N, D) = \begin{cases} \mu_T\left(\frac{N}{D}\right), & \text{for } C \in \left\{N, \frac{N}{2}, \frac{N}{4}\right\} \\ \frac{N}{D}\log_2\frac{N}{D} - \frac{N}{D}, & \text{for } C = \frac{D}{2} \\ \mu_T\left(\frac{N}{D}\right) + \beta^d\left(N, \frac{N}{D}\right), & \text{otherwise} \end{cases} \tag{29}$$

and,

$$\alpha_{GT}^d(N, D) = \begin{cases} \alpha_T\left(\frac{N}{D}\right), & \text{for } C \in \left\{N, \frac{N}{2}, \frac{N}{4}\right\} \\ 3\frac{N}{D}\log_2\frac{N}{D} - \frac{N}{D}, & \text{for } C = \frac{D}{2} \\ \alpha_T\left(\frac{N}{D}\right) + \beta^d\left(N, \frac{N}{D}\right), & \text{otherwise} \end{cases} \tag{30}$$

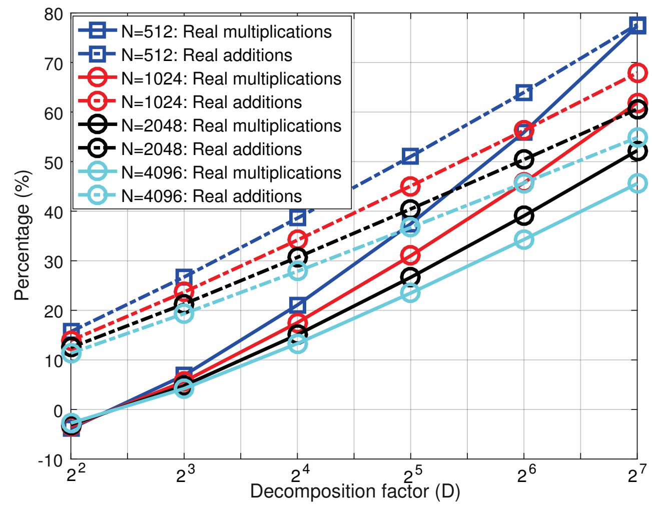

Fig. 6. The reduction percentage in complexity of the narrowband D-FC-FB compared to FC-FB with $N = 512, 1024, 2048$ and 4096.

respectively, where $C = \gcd(N, d)$ and $\gcd(\cdot)$ is the greatest common divisor. The function $\beta^d\left(N, \frac{N}{D}\right)$ returns the number of real multiplications with equal number of additions that are required to multiply a complex sequence by a sequence of $W_N^{k'd}$ where $k' = 0, 1, \ldots, \frac{N}{D} - 1$ and it is defined as follows:

$$\beta^d(N, S) = \begin{cases} 3S - \left\lceil 8S\frac{C}{N} \right\rceil - 2\left\lceil 4S\frac{C}{N} \right\rceil, & \text{for } \frac{N}{C} \notin \{1, 2, 4\} \\ 0, & \text{otherwise} \end{cases}. \tag{31}$$

The computational complexity, normalized to number of processed subcarrier symbols, can be expressed for any FC-FB scheme as

$$\mu = \frac{2\left[\mu^{lg} + \mu^{sh}\right]}{\sum_{b=1}^{B} L_{s,b}} \tag{32}$$

$$\alpha = \frac{2\left[\alpha^{lg} + \alpha^{sh}\right]}{\sum_{b=1}^{B} L_{s,b}} \tag{33}$$

for real multiplications and additions, respectively. Here $\mu^{lg} = \mu_T(N)$ and $\alpha^{lg} = \alpha_T(N)$ for FC-FB and $\mu^{lg} = \mu_D^{lg}$ and $\alpha^{lg} = \alpha_D^{lg}$ for D-FC-FB. The difference in the computational complexity between FC-FB and D-FC-FB is due to the long transforms part and it is expressed as follows:

$$\mu_T(N) - \mu_D^{lg} = \alpha_T(N) - \alpha_D^{lg} = -(D-4)_D. \tag{34}$$

This implies that D-FC-FB scheme has a slightly higher complexity than FC-FB scheme when $D > 4$ and their complexity is equal when $D \in \{2, 4\}$.

Significant reduction in the computational complexity can be achieved in the narrowband D-FC-FB. Again, the differences are due to the long transform part only. Therefore, it is

TABLE I
THE MAXIMUM NUMBER OF USED RBS FOR DIFFERENT DECOMPOSITION FACTORS D.

BW	D				
	8	16	32	64	128
5	5	2	1	–	–
20	21	10	5	2	1

sufficient to represent the complexity for the long transform part which is expressed as follows,

$$\mu_{ND}^{lg} = D\mu_T\Big(\frac{N}{D}\Big) + \sum_{k\in\boldsymbol{K}} \beta_T^k\Big(N, D\Big) \tag{35}$$

$$\alpha_{ND}^{lg} = D\alpha_T\Big(\frac{N}{D}\Big) + \sum_{k\in\boldsymbol{K}} \beta_T^k\Big(N, D\Big) \tag{36}$$

for real multiplications and additions, respectively. Here $\boldsymbol{K} \in \{0, 1, \ldots, N-1\}$ is the set of used frequency points and $\beta_T^d(N, D)$ is the function that returns the number of real multiplications and additions to implement N-DFT with a single input located at index d for output in the period $[0, D-1]$ and it is expressed as follows,

$$\beta_T^d(N, D) = \begin{cases} \frac{N}{2C} - 2, & \text{for } \frac{N}{C} \notin \boldsymbol{N_c}, D \geq \frac{N}{4C} \\ D + \frac{N}{4C} - 2, & \text{for } \frac{N}{C} \notin \boldsymbol{N_c}, \frac{N}{8C} < D < \frac{N}{4C} \\ 3D - 3, & \text{for } \frac{N}{C} \notin \boldsymbol{N_c}, \frac{N}{8C} \geq D \\ 0, & \text{otherwise} \end{cases} \tag{37}$$

where $\boldsymbol{N_c}$ is the set of the numbers $\{1, 2, 4\}$.

VI. NUMERICAL RESULTS

In this section, the computational complexity of the narrowband D-FC-FB scheme is evaluated and compared in different scenarios. First we compare a basic FC-FB with the corresponding narrowband variant of D-FC-FB. The parameters of the FC-FB are $N = \{512, 1024, 2048, 4096\}$, $L = 16$ and $L_s = 12$. To show the worst case scenario of narrowband D-FC-FB, we choose the number of active frequency points to be $\frac{N}{D}$ and these points to be located within the period $[\frac{N}{D}, 2\frac{N}{D}-1]$. The results depicted in Fig. 6 show the superiority of the narrowband D-FC-FB in terms of complexity when $D > 4$. Using the narrowband D-FC-FB, more than 20% of the real multiplications can be saved when $D > 16$. Based on the analysis of Section V, the saving in the computational complexity is rather independent of the overlap factor.

In the second comparison, we consider an FBMC/OQAM system with LTE-like parametrization. Operation with relatively low number of active subcarriers is relevant from the user equipment (UE) point of view. The subcarrier spacing is 15 kHz, and the LTE spectrum is divided into groups of 12 subcarriers that are called resource blocks (RBs). We consider two scenarios with 5 MHz and 20 MHz bandwidths, using 512- and 2048-point IFFTs in the OFDM case, respectively.

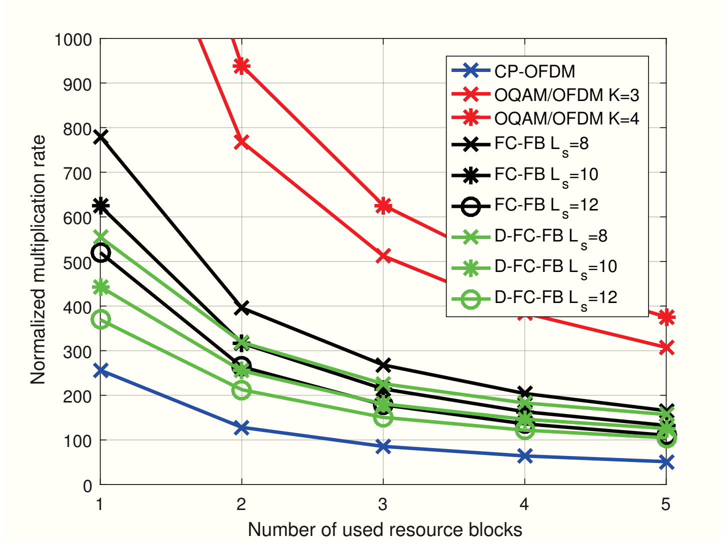

Fig. 7. The normalized number of real multiplications per QAM symbol as a function of the active bandwidth in 5 MHz scenario.

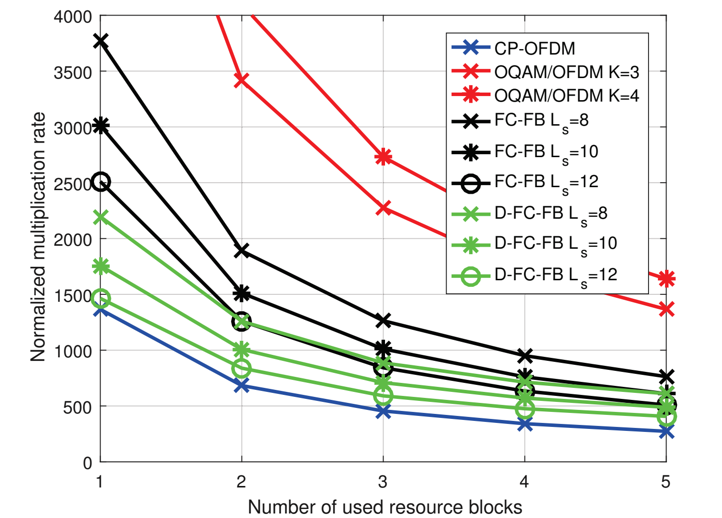

Fig. 8. The normalized number of real multiplications per QAM symbol as a function of the active bandwidth in 20 MHz scenario.

The number of active subcarriers is 300 (25 RBs) or 1200 (100 RBs), correspondingly. The complexity of a CP-OFDM transmitter is used as a reference. As another reference, polyphase filter bank implementations of FBMC/OQAM with overlapping factors of $K = 3$ and $K = 4$ are considered. The complexity of the polyphase FBMC/OQAM is computed according to the complexity analysis of [19].

FC-FB based FBMC/OQAM uses short transforms of size $L = 16$, with alternative non-overlapping lengths of $L_s = \{8, 10, 12\}$, and the long transform of size $N = 4096$ or 16384 for 5 MHz and 20 MHz bandwidths, respectively. For narrowband D-FC-FB, the decomposition factor D is chosen to be greater than 4, following (22). The detailed choices of the decomposition factors are shown in Table I. The active RBs are positioned to start at the FFT bins 841 and 3385 in the 5

MHz and 20 MHz cases, respectively. The normalized number of multiplications per used resource block are depicted in Fig. 7 and Fig. 8 for 5 MHz and 20 MHz scenarios, respectively.

Also in this comparison, the D-FC-FB scheme is superior to both the basic FC-FB based and polyphase filter bank based FBMC/OQAM, in terms of computational complexity. When small number of RBs are used, D becomes larger and the scheme becomes computationally more efficient. The complexity reduction is most significant with small FC overlap factors $1 - L_s/L$. Generally for FC-FB, a small overlap factor gives lower complexity, with the cost of increased out-of-band emission and in-band interference level [20]. The overlap factor should be selected based on the system requirements, together with the other parameters. Generally, the circular interference due to reduced overlap in the FC processing depends on the length of the overlapping parts [18]. Therefore, when the number of FFT bins per subband is increased, smaller overlap factor can be accepted. The in-band interference and out-of-band emission characteristics of FC-FB based FBMC/OQAM were reported in [20] and the D-FC-FB based implementations reach practically the same performance. Even with $L_s = 12$ the in-band signal-to-interference ratio is clearly above 30 dB, which is sufficient for 256-QAM modulation.

VII. Conclusion

This paper developed an effective decomposition scheme for FC-FB based waveform processing on the transmitter side for cases where the active frequency band is narrow compared to the overall carrier bandwidth. Such cases are relevant especially for low-complexity terminal devices, e.g., in machine-type communications. Using the narrowband D-FC-FB structure, it is straightforward to dynamically configure the center frequency of the transmitted group of RBs. If dynamic configuration of the active bandwidth is required, then it is advisable to choose the D-parameter according to the most wideband allocation. Apart from minor differences in finite wordlength effects in practical implementations, the decomposed scheme is perfectly equivalent to the original FC-FB scheme. In realistic narrowband scenarios, 20 - 40 % reduction in multiplication rates was demonstrated.

This approach can equally well be used on the receiver side, using a dual decomposed FC-FB structure. In addition to FBMC/OQAM, the scheme is applicable, in narrowband scenarios, also for other filter bank based multicarrier waveforms, single-carrier waveforms, as well as for filtered OFDM schemes.

The future work based on D-FC-FB will target at evaluating the complexity gains with other waveforms, also on the receiver side. Moreover, the generic cases with non-power-of-two transform lengths will be examined.

References

[1] D. Soldani and A. Manzalini, “Horizon 2020 and beyond: On the 5G operating system for a true digital society,” *IEEE Vehicular Technology Magazine*, vol. 10, no. 1, pp. 32–42, March 2015.

[2] E. Dahlman, S. Parkvall, and J. Sköld, Eds., *4G: LTE/LTE-Advanced for Mobile Broadband (Second Edition)*. Oxford: Academic Press, 2014.

[3] G. Wunder, M. Kasparick, S. ten Brink, F. Schaich, T. Wild, I. Gaspar, E. Ohlmer, S. Krone, N. Michailow, A. Navarro, G. Fettweis, D. Ktenas, V. Berg, M. Dryjanski, S. Pietrzyk, and B. Eged, “5GNOW: Challenging the LTE design paradigms of orthogonality and synchronicity,” in *Proc. IEEE 77th Vehicular Technology Conf. (VTC Spring)*, Dresden, Germany, June 2013, pp. 1–5.

[4] P. Siohan, C. Siclet, and N. Lacaille, “Analysis and design of OFDM/OQAM systems based on filterbank theory,” *IEEE Transactions on Signal Processing*, vol. 50, no. 5, pp. 1170–1183, May 2002.

[5] B. Farhang-Boroujeny, “OFDM versus filter bank multicarrier,” *IEEE Signal Processing Magazine*, vol. 28, no. 3, pp. 92–112, May 2011.

[6] M. Bellanger, “FS-FBMC: An alternative scheme for filter bank based multicarrier transmission,” in *Proc. 5th Int. Symp. on Communications Control and Signal Processing (ISCCSP)*, Rome, Italy, May 2012, pp. 1–4.

[7] M. Renfors and F. Harris, “Highly adjustable multirate digital filters based on fast convolution,” in *Proc. 20th European Conf. on Circuit Theory and Design (ECCTD)*, Linköping, Sweden, Aug 2011, pp. 9–12.

[8] M. Renfors, J. Yli-Kaakinen, and F. J. Harris, “Analysis and design of efficient and flexible fast-convolution based multirate filter banks,” *IEEE Transactions on Signal Processing*, vol. 62, no. 15, pp. 3768–3783, Aug 2014.

[9] J. Yli-Kaakinen and M. Renfors, “Multi-mode filter bank solution for broadband PMR coexistence with TETRA,” in *Proc. 2014 European Conf. on Networks and Communications (EuCNC)*, Bologna, Italy, June 2014, pp. 1–5.

[10] M. Renfors and J. Yli-Kaakinen, “Channel equalization in fast-convolution filter bank based receivers for professional mobile radio,” in *Proc. of 20th European Wireless Conf.*, Barcelona, Spain, May 2014, pp. 1–5.

[11] G. Fettweis, M. Krondorf, and S. Bittner, “GFDM – Generalized frequency division multiplexing,” in *Proc IEEE 69th Vehicular Technology Conference (VTC Spring).*, Barcelona, Spain, April 2009, pp. 1–4.

[12] N. Michailow, I. Gaspar, S. Krone, M. Lentmaier, and G. Fettweis, “Generalized frequency division multiplexing: Analysis of an alternative multi-carrier technique for next generation cellular systems,” in *Proc. Int. Symp. on Wireless Communication Systems (ISWCS)*, Paris, France, Aug 2012, pp. 171–175.

[13] J. Li, K. Kearney, E. Bala, and R. Yang, “A resource block based filtered OFDM scheme and performance comparison,” in *Proc. 20th Int. Conf. on Telecommunications (ICT)*, Casablanca, Morocco, May 2013, pp. 1–5.

[14] M. Renfors, J. Yli-Kaakinen, T. Levanen, M. Valkama, T. Ihalainen, and J. Vihriala, “Efficient fast-convolution implementation of filtered CP-OFDM waveform processing for 5G,” in *Proc. IEEE Globecom Workshops (GC Wkshps)*, San Diego, CA, USA, Dec 2015, pp. 1–7.

[15] R. E. Blahut, *Fast algorithms and multidimensional convolutions*. Cambridge University Press, 006 2010.

[16] H. Sorensen, M. Heideman, and C. Burrus, “On computing the split-radix FFT,” *IEEE Transactions on Acoustics, Speech, and Signal Processing*, vol. 34, no. 1, pp. 152–156, Feb 1986.

[17] J. Yli-Kaakinen and M. Renfors, “Optimization of flexible filter banks based on fast-convolution,” in *Proc. IEEE Int. Conf. on Acoustics, Speech and Signal Processing (ICASSP)*, Florence, Italy, May 2014, pp. 8317–8320.

[18] ——, “Optimization of flexible filter banks based on fast convolution,” *Journal of Signal Processing Systems*, vol. 85, no. 1, pp. 101–111, 2016. [Online]. Available: http://dx.doi.org/10.1007/s11265-015-1004-6

[19] L. G. Baltar, F. Schaich, M. Renfors, and J. A. Nossek, “Computational complexity analysis of advanced physical layers based on multicarrier modulation,” in *Proc. Future Network Mobile Summit (FutureNetw), 2011*, Warsaw, Poland, June 2011, pp. 1–8.

[20] K. Shao, J. Alhava, J. Yli-Kaakinen, and M. Renfors, “Fast-convolution implementation of filter bank multicarrier waveform processing,” in *Proc. IEEE Int. Symp. on Circuits and Systems (ISCAS)*, Lisbon, Portugal, May 2015, pp. 978–981.